

Best sum-throughput evaluation of cooperative downlink transmission nonorthogonal multiple access system

Ahmad Albdairat, Fayez Wanis Zaki, Mohammed Mahmoud Ashour

Department of Electronics and Communications Engineering, Faculty of Engineering, Mansoura University in Egypt, Mansoura, Egypt

Article Info

Article history:

Received Feb 14, 2023

Revised Aug 4, 2023

Accepted Sep 6, 2023

Keywords:

Cell-edge users

Decoding

Nonorthogonal multiple access system

Probability

Sum-throughput analysis

Wireless communication

ABSTRACT

In cooperative simultaneous wireless information and power transfer (SWIPT) nonorthogonal multiple access (NOMA) downlink situations, the current research investigates the total throughput of users in center and edge of cell. We focus on creating ways to solve these problems because the fair transmission rate of users located in cell edge and outage performance are significant hurdles at NOMA schemes. To enhance the functionality of cell-edge users, we examine a two-user NOMA scheme whereby the cell-center user functions as a SWIPT relay using power splitting (PS) with a multiple-input single-output. We calculated the probability of an outage for both center and edge cell users, using closed-form approximation formulas and evaluate the system efficacy. The usability of cell-edge users is maximized by downlink transmission NOMA (CDT-NOMA) employing a SWIPT relay that employs PS. The suggested approach calculates the ideal value of the PS coefficient to optimize the sum throughput. Compared to the noncooperative and single-input single-output NOMA systems, the best SWIPT-NOMA system provides the cell-edge user with a significant throughput gain. Applying SWIPT-based relaying transmission has no impact on the framework's overall throughput.

This is an open access article under the [CC BY-SA](https://creativecommons.org/licenses/by-sa/4.0/) license.



Corresponding Author:

Ahmad Albdairat

Department of Electronics and Communications Engineering, Faculty of Engineering, Mansoura

University in Egypt

Mansoura, Egypt

Email: ahmeddiab2785@yahoo.com

1. INTRODUCTION

To increase the system performance regarding the next gen of wireless network communication technologies, nonorthogonal multiple access (NOMA) has recently appeared as a possible strategy [1]–[4]. The fundamental idea behind NOMA is that, unlike traditional orthogonal multiple access (OMA) systems, There is user multiplexing in the power domain [1]. To illustrate, in a two-user NOMA system, a base station (BS) converses with both users at once while one of them has a worse channel status and is typically placed at the center of cell or close to the BS. Data signals from the two users are mounted at the BS with differing power distributions, with a higher power allocation coefficient for cell-edge users compared to cell-center users. The superposed signal is split at the receiver section using the successive interference cancellation (SIC) methodology [2]. According to previous research [3], under certain conditions, NOMA can outperform OMA and increase throughput by 34.2 at user of the cell edge. Cell center and edge users collaborate and gain by being awarded greater bandwidth when NOMA is used; thus, the spectral efficiency can be greatly increased [4].

According to the current literature, the functioning of NOMA poses the question of rate of data fairness between users at the cell center and edge. The reality that users of cell-edge frequently experience

lower rates than cell-center users makes user throughput fairness a crucial problem [5]. Furthermore, as stated in a previous study [6], if the user of cell edge wants a maximum throughput similar to that of the user of cell center, the power allocation coefficient of the user of cell center should be near to zero. A large portion of the transmitted power is allotted to users of cell edge; thus, it might negatively affect the quality of service of cell-center users. In addition, it could jeopardize the cell-edge users' capacity to receive signals reliably [7]. Therefore, solving the user throughput fairness problem while enhancing the cell-edge user's reception dependability is crucial in the NOMA context.

Using cooperative relaying transmissions is one way to approach this fairness problem while ensuring the efficiency and dependability of the cell-edge user. Previous authors [8] presented a cooperative NOMA transmitting technique wherein cell-center users (with improved channel characteristics) take advantage of historical data already present in the NOMA scheme to increase the reception dependability of cell-edge users (with weak connections to a BS). According to those results [8], cooperative NOMA transmissions improve the outage probability (OP) compared with traditional OMA and noncooperative NOMA systems. Zhang *et al.* [9] demonstrated how cooperative relaying transmissions, in which the cell-center user serves as a relay, may greatly increase the sum rate of NOMA systems. However, a sizable performance disparity still exists between cell-center and cell-edge users.

Another study [10] examined a two user NOMA system where the best user of cell center is chosen to act as a relay to serve a cell-edge user operate better during outages. The problem of how cell-center users equitably spend their energy is posed because they must analyze and transfer their data from the cell-edge users, even if cooperative relaying transmissions are an acceptable approach to overcome the stated problems in NOMA schemes. A novel wireless multiple access technique that is effective in terms of energy and spectrum, the cooperative simultaneous wireless information and power transfer (SWIPT) NOMA protocol, was presented [11] by merging cooperative NOMA and SWIPT. In particular, the study [11] revealed that, in contrast to the traditional cooperative NOMA, the adoption of SWIPT allows the users of cell center to self-power and has no impact on the benefits of variety for users of cell edge.

Time division multiple access and NOMA are wireless protocols used in the downlink scenario [12], whereas in the uplink scenario, NOMA with timeshare is taken into account. Multiple-input, single-output (MISO) system applications of NOMA have also been researched in the literature [13], [14]. Further, it was investigated how the concept of quasi-degradation affected MISO-NOMA downlink communication [13]. A quality-of-service system model was also researched [14] while taking a two-user MISO-NOMA system into account with two objective interference levels. Furthermore, An energy-saving and low-complexity transmission technique for a BS with numerous antennas is called transmit antenna selection (TAS) [15], [16]. Particularly, TAS systems might be a valuable compromise between the variety advantage and installation expense [17]. Nguyen *et al.* [18] created user timetables and antenna selection methods to increase the throughput of multiple-input multiple-output-NOMA networks, in which various selected antennae split users into pairs. Networks with NOMA downlink energy harvesting (EH) multiple antennas were examined using a TAS system [19]. A specialized EH amplify-and-forward relay facilitates the transmission from the sender to receiver, where NOMA is conducted at the relay because the authors expected direct linkages between a source and destination to be prohibited. In this study, a two-user cooperative MISO-NOMA system is considered, in which a cell-center user serves as a relay to facilitate communication from a BS to a cell-edge user. The proposed techniques increase energy efficiency for the cell-center user while enhancing the cell-edge user's performance. To achieve this, we provide cooperative transmission networks where the BS uses TAS criteria, the user of cell center uses SWIPT and the decode-and-forward relaying approach, and the cell-edge user uses selection merging. The following is a summary of the paper's key contributions. The full article follows the standard structure: introduction, system model, outage performance analysis, performance analysis for the optimal sum throughput, numerical results and discussion, and conclusions.

2. SYSTEM MODEL

In Figure 1, we take into account a CDT-NOMA downlink transmission which a BS, represented with S , simultaneously interacts with a user of cell center (user X) and a cell-edge user (user Y) using a two-user NOMA scheme. Each user has a single antenna, whereas the BS has L antennae. We define h_{jK} as the channel fading coefficient from antenna j , $j = \{1, \dots, L\}$ to a user K , where $K \in \{X, Y\}$, and Rayleigh block flat fading is present in every wireless channel in the system, where a complicated independent Gaussian random variable with zero mean and variance $\lambda_{S,L}$ can be used to model h_{jK} . Furthermore, we let n_{aK} and n_{cK} denote the downconverter at user T and the additive white Gaussian noise at the receiving antenna, respectively, with variance σ_{cK}^2 and zero mean σ_{aK}^2 . Thus, the channel gain $|h_{AB}|^2$, where $A \in \{j, X\}$

and $B \in \{X, Y\}$, is an exponential random variable with probability density function $f_{|h_{AB}|^2}(z) = \frac{1}{\lambda_{AB}} e^{-\frac{z}{\lambda_{AB}}}$, $\forall z \geq 0$; otherwise, $z < 0$ and $f_{|h_{AB}|^2}(z) = 0$, where λ_{AB} indicates the mean of $|h_{AB}|^2$. Furthermore, $E[|h_{AB}|^2]$ indicates the average gain of the channel equal to $\frac{l}{(d_{AB}/d_0)^\epsilon}$, where d_{AB} describes the separation between two nodes, ϵ represents the path-loss exponent, the reference distance is specified by d_0 , and l is the average attenuation of the signal power at d_0 . Relay X acts as a hybrid TS/PS EH relay in the presented approach (see [20]–[24] and the references therein for additional information on hybrid TS/PS receivers). Three subblocks of block time T are separated. Relay N initially harvests energy in the first subblock with an αT duration time, where $0 \leq \alpha < 1$ specifies the amount of block time used for EH. Relay N concurrently uses a portion of the received power denoted by ρ for PS and a portion denoted by $(1 - \rho)$ for EH. The remaining portion (denoted by $0 \leq \rho < 1$) is used for data decoding. Relay X uses all captured energy to execute its relaying activity in the final subblock with a $(1 - \rho)T/2$ duration. Figure 2 displays the hybrid TS/PS's timing structure for cooperative relaying communication.

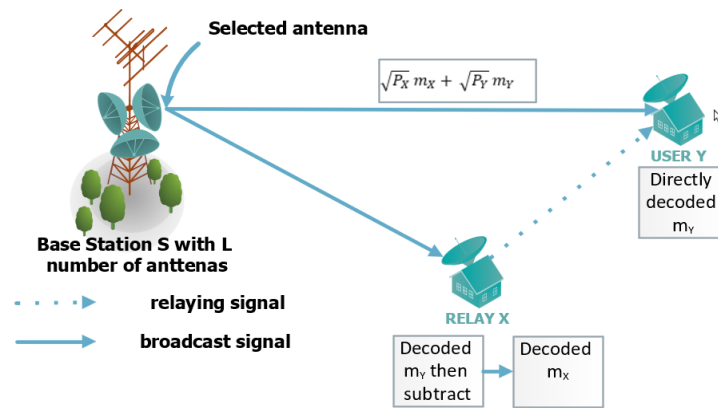


Figure 1. System model

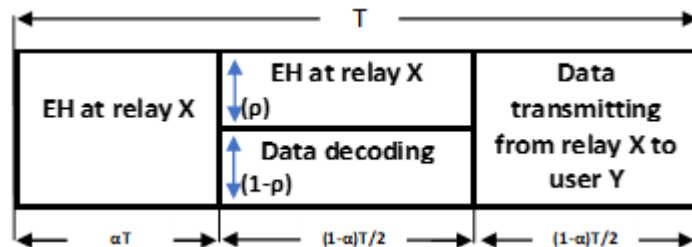


Figure 2. Timing framework of the hybrid TS/PS in cooperative relaying transmission

We assume the hybrid TS/PS SWIPT provides a thorough analysis and creates a generic analytical model for SWIPT design. The hybrid receiver offers broad options for the design process. If TS or PS is not required, then α (or ρ) is set to zero. Given that TS and PS have equal status, it may not matter which phase is completed first [22]. Furthermore, because the data decoding and relaying procedures are sequential, considering TS first makes the temporal structure in Figure 2 more logical. The downlink case of the proposed approach is performed in two stages: the EH and direct data transfer phases, which are required in the first and second subblocks, and the cooperative relaying transfer phase, which is necessary for the third subblock, following the period of the hybrid TS/PS EH protocol in Figure 2. The second and third subblocks have identical lengths.

Furthermore, throughout the final subblock, or the cooperative relaying transfer phase, S remains silent while relay N transmits to user F . The same frequency is used for direct and relaying communications. Therefore, the cell-edge subscriber faces cochannel interference due to the continued broadcast by the BS if relay X continues to relay messages to user Y . Therefore, the direct and relaying transmissions are implemented in two distinct submodules to stop such cochannel interference. The literature has widely

accepted using two independent subblocks, where a relay communicates to a sender while the BS is silent (e.g., [25]–[30]).

2.1. First phase: energy harvesting

We assume that BS antenna j transmits the data. Based on the NOMA concept, the purpose is to send messages m_x and m_y for relay X and user Y , respectively, combined as $\sqrt{P_x m_x} + \sqrt{P_y m_y}$ and transmitted with antenna was chosen at the start of the 1'st subblock period, where P_x and P_y specify the power allocation coefficients for relay X and user Y , respectively. Utilizing the NOMA concept, we presume that $|h_{jX}|^2 > |h_{jY}|^2$, $0 < P_x < P_y$, and $P_x + P_y = 1$.

2.1.1. Relay X

The observation that the antenna for user X can be expressed as (1):

$$y_{jX} = (\sqrt{P_x P_S} m_x + \sqrt{P_y P_S} m_y) h_{jX} + n_{ax}, \quad (1)$$

where $h_{jX} \sim CN(0, \lambda_{SX})$ and $n_{ax} \sim CN(0, \sigma_{ax}^2)$. The overall harvested energy at relay X connected to antenna ii may be stated as follows using the hybrid TS/PS EH technique:

$$E_{jX} = \eta P_S |h_{jX}|^2 \alpha T + \eta \rho P_S |h_{jX}|^2 (1 - \alpha) T / 2, \quad (2)$$

where η represents the efficiency of energy conversion scaled from 0 to 1, the channel gain between relay X and antenna j represented by $|h_{jX}|^2$ for data decoding (DD), The signal that was received at relay X is calculated as (3):

$$y_{jX}^{DD} = \sqrt{1 - \rho} [(\sqrt{P_x P_S} m_x + \sqrt{P_y P_S} m_y) h_{jX} + n_{ax}] + n_{cx}, \quad (3)$$

where $n_{cx} \sim CN(0, \sigma_{cx}^2)$. The SIC receiver at relay X initially decodes m_y based on the NOMA principle, the next step deducts this fraction from the signal that arrives to get the intended information. (i.e., m_x) [31]. To decode this, the received signal to interference plus noise ratio at relay X is

$$\gamma_{jX}^{m_y} = \frac{(1 - \rho) P_y P_S |h_{jX}|^2}{(1 - \rho) P_x P_S |h_{jX}|^2 + (1 - \rho) \sigma_{ax}^2 + \sigma_{cx}^2}, \quad (4)$$

When relay X is used to decode m_x , the received signal-to-noise ratio (SNR) is represented as (5):

$$\gamma_{jX}^{m_x} = \frac{(1 - \rho) P_y P_S |h_{jX}|^2}{(1 - \rho) \sigma_{ax}^2 + \sigma_{cx}^2}. \quad (5)$$

2.1.2. User Y

User Y can execute EH or remain silent in the first subblock and only decode information in the second subblock. Compared to relay X , user Y can decode the data signal because user Y has a greater transmit power allocation; Consequently, interference from relay X 's data transmission might be regarded as noise [32]. To decode m_y using the received SNR at user Y , the observed data may be represented as (6):

$$y_{jY} = (\sqrt{P_x P_S} m_x + \sqrt{P_y P_S} m_y) h_{jY} + n_{ax} + n_{cY}, \quad (6)$$

where $h_{jY} \sim CN(0, \lambda_{SY})$, $n_{aY} \sim CN(0, \sigma_{aY}^2)$, and $n_{cY} \sim CN(0, \sigma_{cY}^2)$, and

$$\gamma_{jY} = \frac{P_y P_S |h_{jY}|^2}{P_x P_S |h_{jY}|^2 + \sigma_{aY}^2 + \sigma_{cY}^2}. \quad (7)$$

2.2. Second phase: direct data-decoded transmission

The following definition can be used to describe the transmit power of relay X in the second phase, assuming that the relaying mechanism is powered entirely by the energy captured during the initial phase, as in [22], [23]. User Y uses the selection combining (SC) approach to merge two signals: the direct signal from the BS and the relaying signal from relay X . Thus, the possible SNR for both signals received combined at user Y can be written as (8):

$$P_X = \frac{E_{jX}}{(1-\alpha)^{T/2}} = \eta P_S |h_{jX}|^2 \left(\frac{2\alpha}{1-\alpha} + \rho \right). \quad (8)$$

The signal received by user F might be described as follows using the decode-and-forward relaying protocol:

$$y_{XY} = (\sqrt{P_X} h_{XY} \hat{m}_Y + n_{aY} + n_{cY}), \quad (9)$$

where $h_{XY} \sim CN(0, \lambda_{XY})$, and the re-encoded form of m_Y is represented by the symbol \hat{m}_Y . The observed SNR at user Y to detect m_Y sent by relay X can be expressed from (8) and (9) as (10), (11)

$$\gamma_{XY} = \frac{\eta P_S |h_{jX}|^2 |h_{jY}|^2 \left(\frac{2\alpha}{1-\alpha} + \rho \right)}{\sigma_{aY}^2 + \sigma_{cY}^2}, \text{ and} \quad (10)$$

$$\gamma_Y^{SC} = \max\{\gamma_{jY}, \gamma_{XY}\}. \quad (11)$$

2.3. Proposed transmit antenna selection criteria

The suggested TAS technique is carried out by the signaling and channel state information (CSI) assessment system prior to data transfer. We presume the necessary CSI for each scheme is available [33], [34]. The ability of m_Y to be decoded at relay X determines whether the cooperative relaying operation succeeds. In light of this, the end-to-end SNR at user Y can be expressed in (12). This approach selects an antenna from L antennae to maximize the instantaneous transmission rate for user Y. The outcome of the scheme selection can be specified formally (14):

$$\gamma_Y^{e2e} = \min\{\gamma_{jX}^{m_X}, \gamma_Y^{SC}\}. \quad (12)$$

When user Y connects to antenna j , the instantaneous transmission rate is represented as (13)

$$R_{jY} = \frac{1-\alpha}{2} \log_2(1 + \gamma_Y^{e2e}), \text{ where} \quad (13)$$

$$j^* = \underset{1 \leq j \leq L}{\operatorname{argmaxmin}}\{\gamma_{jX}^{m_Y}, \max\{\gamma_{jY}, \gamma_{XY}\}\}. \quad (14)$$

3. OUTAGE PERFORMANCE ANALYSIS

The OP is a probability that the information rate will go under the required threshold rate for data [35]. Assuming $R_{th,X}$ and $R_{th,Y}$ indicate the desired data rates in bits/s/Hz for relay X and Y, respectively:

$$a_1 \triangleq \frac{(1-\rho)P_Y P_S}{(1-\rho)\sigma_{aX}^2 + \sigma_{cX}^2}, a_2 \triangleq \frac{(1-\rho)P_X P_S}{(1-\rho)\sigma_{aX}^2 + \sigma_{cX}^2}, b_1 \triangleq \frac{P_Y P_S}{\sigma_{aY}^2 + \sigma_{cY}^2}, b_2 \triangleq \frac{P_X P_S}{\sigma_{aY}^2 + \sigma_{cY}^2},$$

$$c \triangleq \eta P_S \left(\frac{2\alpha}{1-\alpha} + \rho \right) / (\sigma_{aY}^2 + \sigma_{cY}^2), \mu_a \triangleq \frac{\gamma_2}{a_1 - a_2 \gamma_2}, \mu_b \triangleq \frac{\gamma_2}{b_1 - b_2 \gamma_2}, \text{ and } \theta \triangleq \frac{P_Y}{P_X}.$$

Function $\Omega(\mu, X, \xi)$ is described in (21). The suggested scheme's OP for relay X and user Y can be stated as:

3.1. Outage probability of relay X

When the SIC process is unable to correctly decode the message m_Y or when m_Y is correctly decoded but m_X is not, outage events happen at user N. Thus, the OP of relay X may be written as (15)

$$OP_X = \Pr(\gamma_{SX}^{m_Y} < \gamma_2) + \Pr(\gamma_{SX}^{m_Y} \geq \gamma_2, \gamma_{SX}^{m_X}), \quad (15)$$

where $\gamma_1 \triangleq 2^{2R_{th,X} - 1}$ and $\gamma_2 \triangleq 2^{2R_{th,X} - 1}$ represent the corresponding thresholds of SNR for messages successfully decoded m_X and m_Y . The OP of relay X for the closed-form equation can be expressed as (16)

$$OP_X = \left\{ 1 - e^{-\frac{\mu_a}{\lambda_{SX}}} \text{ if } \gamma_2 < \theta, \mu_a \geq \frac{\gamma}{a_2} \quad 1 - e^{-\frac{\gamma_1}{\lambda_{SX} a_2}} \text{ if } \gamma_2 < \theta, \mu_a \geq \frac{\gamma}{a_2} \quad 1 \text{ if } \gamma_2 \geq \theta, \forall \gamma_1. \right. \quad (16)$$

The OP of relay X may be written from (4), (5), and (12) as

$$OP_X = Pr\left(\frac{a_1|h_{SX}|^2}{a_2|h_{SX}|^2+1} < \gamma_2\right) + Pr\left(\frac{a_1|h_{SX}|^2}{a_2|h_{SX}|^2+1} \geq \gamma_2, a_2|h_{SX}|^2 < \gamma_1\right). \quad (17)$$

It is apparent that $Pr\left(\frac{a_1|h_{SX}|^2}{a_2|h_{SX}|^2+1} < \gamma_2\right) = Pr\left((a_1 - a_2\gamma_2)|h_{SX}|^2 < \gamma_2\right)$ is equal to 1 if $\gamma_2 \geq \theta$, where $\theta = \frac{a_1}{a_2}$. Therefore, the OP closed-form equation of relay X may be obtained using specific algebraic methods using certain algebraic operations to examine the relative connections between γ_1, γ_2 , and θ , as presented in (13).

3.2. Outage probability for user Y

Message m_Y for user Y is decoded at user Y and in the SIC process at relay X , as observed in the first phase of the system model. The SIC process connected to m_Y is already considered in the formulation of γ_Y^{e2e} in (11). Consequently, the user Y 's OP could be expressed as (18)

$$OP_Y = Pr(\min\{\gamma_{SX}^{m_Y}, \max\{\gamma_{SY}, \gamma_{XY}\}\} < \gamma_2), \quad (18)$$

where the threshold of SNR for successfully message decoded m_Y is denoted by $\gamma_2 \triangleq 2^{2R_{th,Y}} - 1$. The following is an approximate closed form expression of user Y 's OP:

$$OP_Y = 1 - \left[1 - e^{\frac{\mu_b}{\lambda_{SY}}}\right] - e^{-\frac{\mu_a}{\lambda_{SX}} - \frac{\mu_b}{\lambda_{SY}}} \times \left[e^{\frac{\mu_b}{\lambda_{SX}}} - \frac{\gamma_2}{c\lambda_{SY}\lambda_{SX}} \Gamma\left(0, \frac{\mu_a}{\lambda_{SX}}\right)\right] \quad (19)$$

$$OP_Y = Pr Pr(R_{jY} < R_{th,Y}) = Pr Pr\left(\max_{1 \leq j \leq L} \{\gamma_{jX}^{m_Y}, \{\gamma_{jY}, \gamma_{XY}\}\} < \gamma_2\right) \quad (20)$$

where the SNR threshold for successfully decoding message m_Y is represented by $m_X, \gamma \triangleq 2^{2R_{th,Y}/(1-\alpha)}$.

4. PERFORMANCE ANALYSIS FOR THE OPTIMAL SUM THROUGHPUT

At this stage, we perform an optimum evaluation of the sum throughput, or τ , of the NOMA approaches explored for downlink case. We specifically offer a way to determine the optimal value of ρ , indicated by ρ^{opt} , which maximizes the sum throughput of the network, which is possible to written as (21).

$$\tau = (1 - OP_X)R_{th,X} + (1 - OP_Y)R_{th,Y} = R_{th,X}e^{-\frac{\mu_a}{\lambda_{SX}}} + R_{th,Y}\left[e^{-\frac{\mu_a}{\lambda_{SX}} - \frac{\mu_b}{\lambda_{SY}}} + (1 - e^{-\frac{\mu_b}{\lambda_{SY}}}) \times \left[e^{-\frac{\mu_a}{\lambda_{SX}}} - \frac{\gamma_2}{\gamma_{SX}\gamma_{XY}c} \Gamma\left(0, \frac{\mu_a}{\lambda_{SX}}\right)\right]\right]. \quad (21)$$

We describe the issue under consideration as an unrestricted optimization problem, defined as (22)

$$\max_{\rho} \tau = f(\rho), \quad (22)$$

where $f(\rho): g(\rho): (0,1) \rightarrow R^+$, and R^+ stands for the collection of positive real numbers. To make the analysis of τ as easy as possible to simplify $g(\rho)$, we assume that $(1 - \rho)n_{aX} \approx n_{aX}$ because the noise power that an antenna introduces is low. For notational simplicity, we let $\underline{\gamma}_X = P_S/(n_{aX} + n_{cX})$ and $\underline{\gamma}_Y = P_S/(n_{aY} + n_{cY})$. Therefore, $g(\rho)$ can be represented as (23)

$$g(\rho) = g_j(\rho) = r_1 e^{\frac{v_i}{1-\rho}} + r_2 e^{\frac{\kappa_a + \kappa_b}{1-\rho}} + r_2 e^{\frac{\kappa_a}{1-\rho}} + \frac{r_2 \kappa_c}{\rho} \Gamma\left(0, -\frac{\kappa_a}{1-\rho}\right), \quad (23)$$

where $j=1$ if $\frac{\gamma_2}{P_Y - P_X \gamma_2} \geq \frac{\gamma_1}{P_X}$, $j=2$ where $r_1 = -R_{th,X}, r_2 = -R_{th,Y}, v_1 = -\frac{\gamma_1}{(P_Y - P_X \gamma_2)\underline{\gamma}_X \lambda_{SX}}, v_2 = -\frac{\gamma_1}{P_X \underline{\gamma}_X \lambda_{SX}}, \kappa_a = -\frac{\gamma_2}{(P_Y - P_X \gamma_2)\underline{\gamma}_X \lambda_{SX}}, \kappa_b = -\frac{\mu_b}{\lambda_{SX}}, \kappa_c = -\frac{\gamma_2}{\lambda_{SX} \lambda_{XY} \eta \underline{\gamma}_Y}, = 1 - e^{-\frac{\mu_b}{\lambda_{SY}}}$.

As observed, $g(\rho)$ has a very complex representation, making it difficult to perform an optimum analysis on this function. We use the gradient descent approach [12] in this study to address the specified issue. In particular, we propose the following simple yet effective technique for locating the ideal PS coefficient. We write the optimal structure of this PS coefficient as ρ^{opt} . The goal is to create a minimizing sequence: $\rho^0, \rho^1, \dots, \rho^k, \dots \in \text{domain } g$ with $g(\rho^k) \rightarrow g(\rho^{opt})$ as $k \rightarrow \infty$, where,

$$\rho^{\kappa+1} = \rho^{\kappa} + t^{\kappa} \Delta \rho^{\kappa}, \quad (24)$$

where κ indicates the iteration number, t^{κ} denotes the step length, and $\Delta \rho^{\kappa}$ represents a search direction step.

We selected a search vector which is the negative gradient of the function using the gradient decrease approach $\Delta \rho^{\kappa} = -\nabla g \rho^{\kappa}$, resulting in $g \rho^{\kappa+1} < g \rho^{\kappa}$. Until the halting requirement is met, the algorithm continues to execute (i.e., $\|\nabla g \rho^{\kappa+1}\|_2 \leq \zeta$, where ζ identifies a stopping threshold and $\|\cdot\|_2$ implies l_2 -norm). In equation (19), the gradient of the desired function may be represented as in technique 1, which provides more information about the proposed algorithm:

$$g(\rho) = \frac{r_1 v_j e^{\frac{v_j}{1-\rho}}}{(1-\rho)^2} + \frac{r_2 \kappa_a e^{\frac{\kappa_a}{1-\rho} + \kappa_b}}{(1-\rho)^2} + \frac{r_2 \zeta \kappa_a e^{\frac{\kappa_a}{1-\rho}}}{(1-\rho)^2} - \frac{r_2 \zeta \kappa_c e^{\frac{\kappa_c}{1-\rho}}}{(1-\rho)\rho} - \frac{r_2 \kappa_c \zeta}{\rho^2} \Gamma\left(0, -\frac{\kappa_a}{1-\rho}\right). \quad (25)$$

The proposed technique allows for off-line optimization depending on the system characteristics obtained through the estimate procedure for CSI (and in advance of the data transfer).

5. RESULTS AND DISCUSSION

This part presents the representative numerical results to check the designed evaluation and show the reachable performance improvement of the ideal SWIPT-NOMA system in contrast to traditional OMA or noncooperative NOMA systems and the PS-based SWIPT relay [36]. During the simulation setup, considering that the source, $N=X$ and $F=Y$ users constitute a line network [37]–[40]. We also assumed the following:

- The antenna noise power density is -100 dBm/Hz, and the bandwidth is 1 MHz,
- The information-processing noise power density is -90 dBm/Hz,
- The selected desired data rate is 1 bit/s/Hz, and user X (P_X) (power allocation coefficient) value is 0.1,
- User Y 's power allocation coefficient is $1-P_X$,
- S is located 10 meters away from user X ,
- User Y and S are 3 meters apart,
- User X and Y are separated by $d_{SY}-d_{SX}$,
- The path-loss exponent is 3,
- The path loss at the reference distance is -30 dB, and
- The EH process has a 0.70 energy conversion efficiency.

We define the OP's of users N and F as a function of the transmit power PS (dB) and the PS coefficient, respectively, of the source in Figures 3 and 4. These two figures illustrate a clear agreement between the analytical and simulation results, demonstrating the accuracy of the established methodology. Additionally, even in low SNR conditions, such as when PS is minimal, the approximate OP for user F remains close to its actual value.

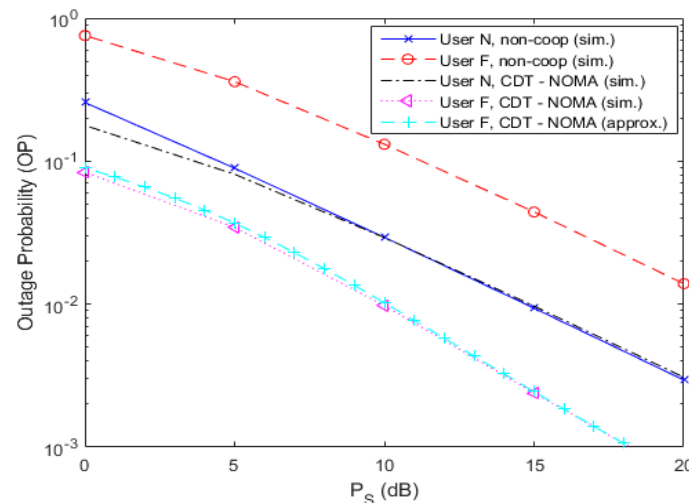


Figure 3. Outage probability for users N and F , following the signal strength at the sender when $\rho=0.3$

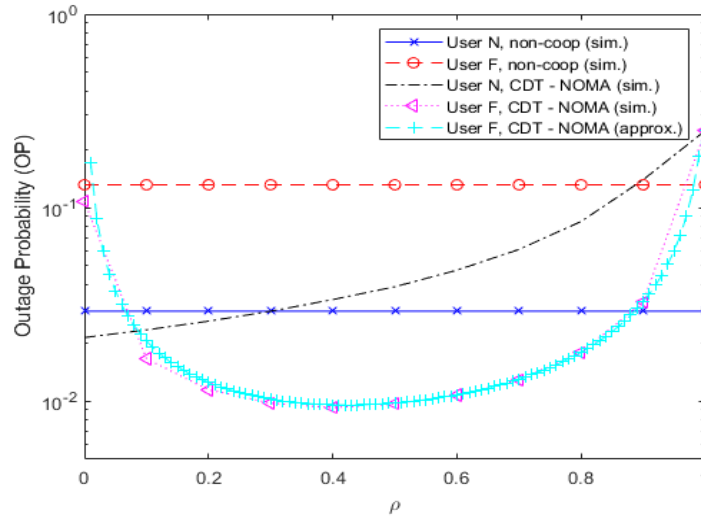


Figure 4. Outage probability for users *N* and *F* as a function of the power-splitting coefficient (PS=10 dB)

In traditional noncooperative NOMA systems, the cell-center user beats the cell-edge user, as presented in Figures 3 and 4. We can still enhance the cell-edge user’s OP by applying a SWIPT-cooperative relaying transfer. Therefore, the OP for user *N* has decreased and is inferior to that for user *F* for a specific value of PS. The reality that user *N* acts as an RF EH relay may be a factor. Specifically, some of the power it receives is used to transmit information, lowering the received SNR of user *N*.

Figure 5 presents the outcome of the proposed methodology for locating the ideal PS coefficient. As observed, the sum throughput is a curved function regarding the PS coefficient. Additionally, the objective function’s relaxed value is quite close to its real value. We compared the performance of the traditional OMA, noncooperative NOMA, and optimal SWIPT-NOMA systems in Figure 6. In the beginning considered the combined throughput (bits/s/Hz) of the described three systems.

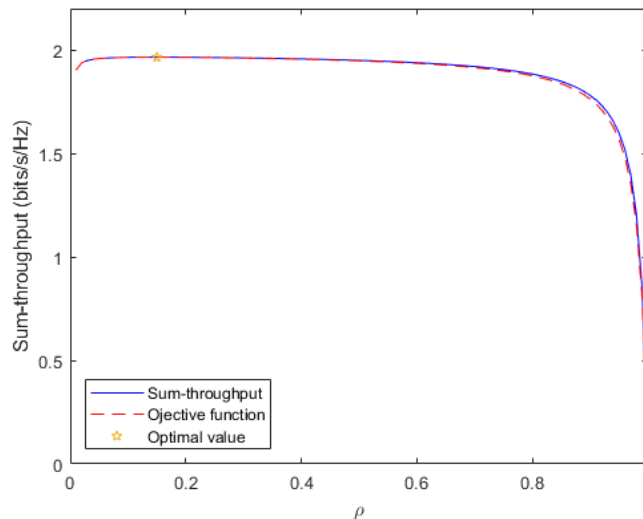


Figure 5. Advantage of the ideal value using the suggested technique when PS=10 dB

The benefit of NOMA with respect to throughput enhancement is confirmed by the fact that the ideal SWIPT-NOMA and noncooperative NOMA systems produce a superior sum throughput compared with the traditional OMA system. Unexpectedly, the possible sum throughputs of the noncooperative NOMA and the best SWIPT-NOMA are comparable. Only one-half of a block period is spent using the NOMA transmission when SWIPT-based relaying is used in the SWIPT-NOMA system. The BS transmits NOMA

data for the full block time in a noncooperative NOMA system. Due to the calculated values, we can conclude that the sum throughput of the two-user NOMA system under consideration is not jeopardized by the SWIPT-based relaying transmission by user N to aid user F . In contrast, the throughput of user F in the best SWIPT-NOMA system is greater than that of the cell-edge user in the noncooperative NOMA system, as illustrated in Figure 6. It implies that the throughput of cell-edge users in NOMA systems is increased using cooperative relaying transmissions.

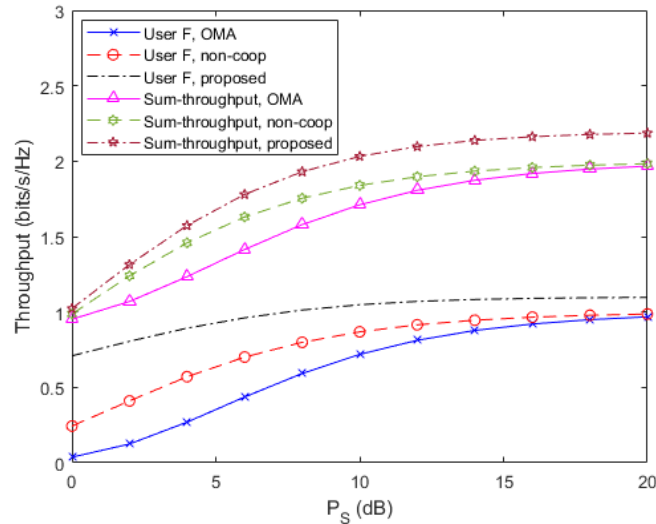


Figure 6. Comparisons of the OMA, noncooperative NOMA, and proposed NOMA systems for performance

6. CONCLUSION

This research investigated the OP and sum throughput of the cooperative PS-based SWIPT two-user NOMA system. We applied the tight closed-form approximation expression for the OP of the cell-edge user and the closed-form expression for the cell-center user. To discover the ideal PS coefficient value that maximizes the sum throughput of the system under consideration, we suggested an approach employing the gradient descent technique. According to the numerical findings, using a cooperative SWIPT relaying transmission with an ideal PS coefficient can increase throughput for cell-edge users without endangering the sum throughput of two-user NOMA systems. Thus, cooperative SWIPT relaying transmissions may be considered a long-term fix for the problems of performance equity between cell-center and cell-edge users and energy usage equity for cell-center users.

REFERENCES




- [1] R. Ramesh, S. Gurugopinath, and S. Muhaidat, "Three-user cooperative dual-stage non-orthogonal multiple access for power line communications," *IEEE Open Journal of the Communications Society*, vol. 4, pp. 184–196, 2023, doi: 10.1109/OJCOMS.2023.3234981.
- [2] Y. Saito, Y. Kishiyama, A. Benjebbour, T. Nakamura, A. Li, and K. Higuchi, "Non-orthogonal multiple access (NOMA) for cellular future radio access," in *2013 IEEE 77th Vehicular Technology Conference (VTC Spring)*, Jun. 2013, pp. 1–5, doi: 10.1109/VTCSpring.2013.6692652.
- [3] R. Gupta and I. Krikidis, "Simultaneous wireless power transfer and modulation classification," in *2021 IEEE 93rd Vehicular Technology Conference (VTC2021-Spring)*, Apr. 2021, pp. 1–6, doi: 10.1109/VTC2021-Spring51267.2021.9448896.
- [4] T. Shimojo, A. Umesh, D. Fujishima, and A. Minokuchi, "Special articles on 5G technologies toward 2020 deployment," *NTT DOCOMO Tech. J.*, vol. 17, no. 4, pp. 50–59, 2016.
- [5] K. Wang *et al.*, "Task offloading with multi-tier computing resources in next generation wireless networks," *IEEE Journal on Selected Areas in Communications*, vol. 41, no. 2, pp. 306–319, Feb. 2023, doi: 10.1109/JSAC.2022.3227102.
- [6] S. Norouzi, B. Champagne, and Y. Cai, "Joint optimization framework for user clustering, downlink beamforming, and power allocation in MIMO NOMA systems," *IEEE Transactions on Communications*, vol. 71, no. 1, pp. 214–228, Jan. 2023, doi: 10.1109/TCOMM.2022.3222374.
- [7] T.-V. Nguyen, V.-D. Nguyen, D. B. da Costa, and B. An, "Hybrid user pairing for spectral and energy efficiencies in multiuser MISO-NOMA networks with SWIPT," *IEEE Transactions on Communications*, vol. 68, no. 8, pp. 4874–4890, Aug. 2020, doi: 10.1109/TCOMM.2020.2994204.
- [8] P. Swami and V. Bhatia, "NOMA for 5G and beyond wireless networks," in *Signals and Communication Technology*, Springer International Publishing, 2023, pp. 143–166.
- [9] G. Zhang *et al.*, "Hybrid time-switching and power-splitting EH relaying for RIS-NOMA downlink," *IEEE Transactions on Cognitive Communications and Networking*, vol. 9, no. 1, pp. 146–158, Feb. 2023, doi: 10.1109/TCCN.2022.3216406.

- [10] A. Mukherjee, P. Chakraborty, S. Prakriya, and A. K. Mal, "Cooperative mode switching-based cognitive NOMA with transmit antenna and user selection," *IEEE Transactions on Signal and Information Processing over Networks*, vol. 8, pp. 932–945, 2022, doi: 10.1109/TSIPN.2022.3223808.
- [11] Z. Ding *et al.*, "A state-of-the-art survey on reconfigurable intelligent surface-assisted non-orthogonal multiple access networks," *Proceedings of the IEEE*, vol. 110, no. 9, pp. 1358–1379, Sep. 2022, doi: 10.1109/JPROC.2022.3174140.
- [12] J. Tang *et al.*, "Joint power allocation and splitting control for SWIPT-enabled NOMA systems," *IEEE Transactions on Wireless Communications*, vol. 19, no. 1, pp. 120–133, Jan. 2020, doi: 10.1109/TWC.2019.2942303.
- [13] L. Liu and J. Zhang, "Performance analysis of MISO-NOMA systems with different antenna selection schemes," in *Advances in Natural Computation, Fuzzy Systems and Knowledge Discovery*, Springer International Publishing, 2022, pp. 1206–1215.
- [14] H. Al-Obiedollah, K. Cumanan, J. Thiyagalingam, A. G. Burr, Z. Ding, and O. A. Dobre, "Energy efficiency fairness beamforming designs for MISO NOMA systems," in *2019 IEEE Wireless Communications and Networking Conference (WCNC)*, Apr. 2019, pp. 1–6, doi: 10.1109/WCNC.2019.8886009.
- [15] T. N. Do, D. B. da Costa, T. Q. Duong, and B. An, "Improving the performance of cell-edge users in MISO-NOMA systems using TAS and SWIPT-based cooperative transmissions," *IEEE Transactions on Green Communications and Networking*, vol. 2, no. 1, pp. 49–62, Mar. 2018, doi: 10.1109/TGCN.2017.2777510.
- [16] T. Wu, Y. Zou, and Y. Jiang, "Secrecy throughput optimization and precoding design in adaptive transmit antenna selection systems with limited feedback," *IEEE Transactions on Vehicular Technology*, vol. 71, no. 11, pp. 11693–11702, Nov. 2022, doi: 10.1109/TVT.2022.3190681.
- [17] P. Yan, J. Yang, M. Liu, J. Sun, and G. Gui, "Secrecy outage analysis of transmit antenna selection assisted with wireless power beacon," *IEEE Transactions on Vehicular Technology*, vol. 69, no. 7, pp. 7473–7482, Jul. 2020, doi: 10.1109/TVT.2020.2992766.
- [18] M.-S. Van Nguyen, D.-T. Do, S. Al-Rubaye, S. Mumtaz, A. Al-Dulaimi, and O. A. Dobre, "Exploiting impacts of antenna selection and energy harvesting for massive network connectivity," *IEEE Transactions on Communications*, vol. 69, no. 11, pp. 7587–7602, Nov. 2021, doi: 10.1109/TCOMM.2021.3106099.
- [19] Q. Wang, J. Ge, Q. Li, and Q. Bu, "Performance analysis of NOMA for multiple-antenna relaying networks with energy harvesting over Nakagami-m fading channels," in *2017 IEEE/CIC International Conference on Communications in China (ICCC)*, Oct. 2017, pp. 1–5, doi: 10.1109/ICCCChina.2017.8330521.
- [20] X. Wu, L. Tang, and J. Yang, "Outage performance of power beacon-assisted cooperative hybrid decode-amplify-forward relaying wireless communications," in *2020 IEEE/CIC International Conference on Communications in China (ICCC)*, Aug. 2020, pp. 1330–1335, doi: 10.1109/ICCC49849.2020.9238898.
- [21] K. Zhong and L. Fu, "Optimal throughput of the full-duplex two-way relay system with energy harvesting," in *2021 IEEE 94th Vehicular Technology Conference (VTC2021-Fall)*, Sep. 2021, pp. 1–6, doi: 10.1109/VTC2021-Fall52928.2021.9625087.
- [22] S. Atapattu and J. Evans, "Optimal energy harvesting protocols for wireless relay networks," *IEEE Transactions on Wireless Communications*, vol. 15, no. 8, pp. 5789–5803, Aug. 2016, doi: 10.1109/TWC.2016.2569097.
- [23] R. Tao, A. Salem, and K. A. Hamdi, "Adaptive relaying protocol for wireless power transfer and information processing," *IEEE Communications Letters*, vol. 20, no. 10, pp. 2027–2030, Oct. 2016, doi: 10.1109/LCOMM.2016.2593877.
- [24] D. L. Galappaththige, R. Shrestha, and G. A. A. Baduge, "Exploiting cell-free massive MIMO for enabling simultaneous wireless information and power transfer," *IEEE Transactions on Green Communications and Networking*, vol. 5, no. 3, pp. 1541–1557, Sep. 2021, doi: 10.1109/TGCN.2021.3090357.
- [25] A. A. Saeed and M. A. Ahmed, "Cognitive radio based NOMA for the next generations of wireless communications," in *2022 International Conference on Electrical Engineering and Informatics (ICELTICs)*, Sep. 2022, pp. 125–130, doi: 10.1109/ICELTICs56128.2022.9932105.
- [26] D. N. Amudala, B. Kumar, and R. Budhiraja, "Spatially-correlated rician-faded multi-relay multi-cell massive MIMO NOMA systems," *IEEE Transactions on Communications*, vol. 70, no. 8, pp. 5317–5335, Aug. 2022, doi: 10.1109/TCOMM.2022.3180066.
- [27] W. Ruoxi, H. Beshley, Y. Lingyu, O. Urikova, M. Beshley, and O. Kuzmin, "Industrial 5G private network: architectures, resource management, challenges, and future directions," in *2022 IEEE 16th International Conference on Advanced Trends in Radioelectronics, Telecommunications and Computer Engineering (TCSET)*, Feb. 2022, pp. 780–784, doi: 10.1109/TCSET55632.2022.9766945.
- [28] T. Xiao *et al.*, "Research on coverage ability assessment of high and low frequency based on machine learning," in *2021 International Conference on Information and Communication Technologies for Disaster Management (ICT-DM)*, Dec. 2021, pp. 86–92, doi: 10.1109/ICT-DM52643.2021.9664166.
- [29] M. D. M. Valadao, W. S. S. Junior, and C. B. Carvalho, "Trends and challenges for the spectrum efficiency in NOMA and MIMO based cognitive radio in 5G networks," in *2021 IEEE International Conference on Consumer Electronics (ICCE)*, Jan. 2021, pp. 1–4, doi: 10.1109/ICCE50685.2021.9427695.
- [30] X. Zhang, L. Yang, Z. Ding, J. Song, Y. Zhai, and D. Zhang, "Sparse vector coding-based multi-carrier NOMA for in-home health networks," *IEEE Journal on Selected Areas in Communications*, vol. 39, no. 2, pp. 325–337, Feb. 2021, doi: 10.1109/JSAC.2020.3020679.
- [31] H. Hanane, M. S. Mohammed, and D. Fouad, "Achievable capacity analysis for power domain non-orthogonal multiple access scheme," in *2022 2nd International Conference on Advanced Electrical Engineering (ICAEE)*, Oct. 2022, pp. 1–4, doi: 10.1109/ICAEE53772.2022.9961969.
- [32] U. Sharma, P. Singh, and M. Awasthi, "Non-orthogonal multiple access (NOMA) for 5G radio technology," in *Proceedings of Third Doctoral Symposium on Computational Intelligence*, Springer Nature Singapore, 2023, pp. 523–532.
- [33] Z. Ding, M. Peng, and H. V. Poor, "Cooperative non-orthogonal multiple access in 5G systems," *IEEE Communications Letters*, vol. 19, no. 8, pp. 1462–1465, Aug. 2015, doi: 10.1109/LCOMM.2015.2441064.
- [34] Y. Liu, Z. Ding, M. ElKashlan, and H. V. Poor, "Cooperative non-orthogonal multiple access with simultaneous wireless information and power transfer," *IEEE Journal on Selected Areas in Communications*, vol. 34, no. 4, pp. 938–953, Apr. 2016, doi: 10.1109/JSAC.2016.2549378.
- [35] A. Goldsmith, *Wireless communications*. Cambridge University Press, 2005.
- [36] T. N. Do and B. An, "Optimal sum-throughput analysis for downlink cooperative SWIPT NOMA systems," in *2018 2nd International Conference on Recent Advances in Signal Processing, Telecommunications & Computing (SigTelCom)*, Jan. 2018, pp. 85–90, doi: 10.1109/SIGTELCOM.2018.8325811.
- [37] S. Kurma, P. K. Sharma, K. Singh, S. Mumtaz, and C.-P. Li, "URLLC-based cooperative industrial IoT networks with nonlinear energy harvesting," *IEEE Transactions on Industrial Informatics*, vol. 19, no. 2, pp. 2078–2088, Feb. 2023, doi: 10.1109/TII.2022.3166808.




- [38] N. T. Do, D. B. da Costa, T. Q. Duong, V. N. Q. Bao, and B. An, "Exploiting direct links in multiuser multirelay SWIPT cooperative networks with opportunistic scheduling," *IEEE Transactions on Wireless Communications*, vol. 16, no. 8, pp. 5410–5427, Aug. 2017, doi: 10.1109/TWC.2017.2710307.
- [39] S. Ozyurt, A. F. Coskun, S. Buyukcorak, G. Karabulut Kurt, and O. Kucur, "A survey on multiuser SWIPT communications for 5G+," *IEEE Access*, vol. 10, pp. 109814–109849, 2022, doi: 10.1109/ACCESS.2022.3212774.
- [40] A. K. Shukla, J. Sharanya, K. Yadav, and P. K. Upadhyay, "Exploiting SWIPT-enabled IoT-based cognitive nonorthogonal multiple access with coordinated direct and relay transmission," *IEEE Sensors Journal*, vol. 22, no. 19, pp. 18988–18999, Oct. 2022, doi: 10.1109/JSEN.2022.3198627.

BIOGRAPHIES OF AUTHORS






Ahmad Albairat    received the B.Eng. degree in communication engineering from University of Mut'ah, Jordan, in 2007 and the M.S. degree in communication engineering from University of Mut'ah, Jordan, in 2011. Currently, he is Jordanian Customs-Amman Customs House Appraiser (Customs Valuation Officer) and Auditor. He can be contacted at email: ahmeddiab2785@yahoo.com.



Fayez Wanis Zaki    is a professor at the Faculty of Engineering, Mansoura University. He received the B.Sc. in communication engineering from Menofia University Egypt 1969, M.Sc. communication engineering from Helwan University Egypt 1975, and Ph.D. from Liverpool University 1982. Worked as a demonstrator at Mansoura University, Egypt from 1969, lecture assistant from 1975, a lecturer from 1982, associate prof. from 1988, and prof. from 1994. Head of Electronics and Communication Engineering Department Faculty of Engineering, Mansoura University from 2002 till 2005. He supervised several M.Sc. and Ph.D. thesis. He has published several papers in refereed journals and international conferences. He is now a member of the professorship promotion committee in Egypt. He can be contacted at email: fwzaki2017@gmail.com.



Mohammed Mahmoud Ashour    is an assistant professor at the Faculty of Engineering Mansoura University, Egypt. He received B.Sc. from Mansoura University Egypt in he received an M.Sc. degree from Mansoura University, Egypt in 1996. He receives a Ph.D. degree from Mansoura University, Egypt 2005. Worked as lecturer assistant at Mansoura University, Egypt from 1997, from 2005, an assistant professor. Fields of interest: network modelling and security, wireless communication, and digital signal processing. He can be contacted at email: mohmoh2@yahoo.com.